ACS Partner Journal
PRECISION CHEMISTRY
pubs.acs.org/PrecisionChem

Letter

Robust Hydrogen-Bonded Organic Framework with Four-Fold Interpenetration for Adsorptive Separation of C_2H_6/C_2H_4 and Xe/Kr

Fu-An Guo, Kang Zhou, Jiaqi Liu, Hao Wang,* and Jing Li*

Cite This: *Precis. Chem.* 2023, 1, 524−529

Read Online

ACCESS | Metrics & More | Article Recommendations | Supporting Information

ABSTRACT: Hydrogen-bonded organic frameworks (HOFs) are an emerging class of porous materials that hold promise for the adsorptive separation of industrially relevant gas mixtures. However, developing HOFs with high thermal stability and resistance to water remains a daunting challenge. We report here a microporous HOF (HIAM-103) assembled from a hexacarboxylate linker (2,4,6-trimethylbenzene-1,3,5-triylisophthalic acid, H_6TMBTI). The compound crystallizes in the trigonal crystal system, and its structure is a four-fold interpenetrated network. Upon thermal activation, the single crystals remain intact, allowing for precise determination of the activated structure. HIAM-103 exhibits remarkable thermal and hydrothermal stability. Its microporous channels demonstrate selective adsorption of C_2H_6 over C_2H_4 and Xe over Kr, and its separation capability toward mixed gases has been validated by column breakthrough experiments under dry and humid conditions. The preferential gas adsorption sites and separation mechanisms have been uncovered through DFT analysis, which suggests that the methyl group decorated 1D channels are the primary reason for the selective adsorption.

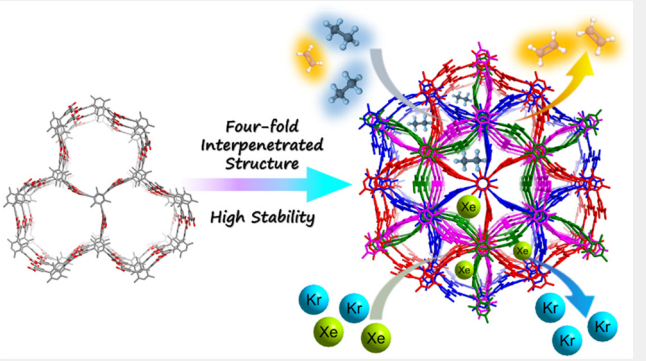

KEYWORDS: *Hydrogen-Bonded Organic Frameworks, Interpenetration, Adsorption, Separation, Selectivity*

Adsorptive separation of light hydrocarbons such as olefin/paraffin and noble gases such as Xe/Kr represents a very important process in petrochemical industry, as such a separation technique can potentially lower the energy consumption and suppress carbon emission associated with the current heat-driven distillations.[1,2] However, the high similarity in physicochemical properties of the gases to be separated makes this process challenging. It is thus crucial to develop adsorbents with tailored pore structure and surface functionality to achieve efficient separation through selective adsorption.[3] While a variety of porous materials have been investigated for the separation of these gases, including activated carbons, zeolites etc.,[4−7] high-performance adsorbents that meet the industrial standard are still lacking. Parallel to zeolites and metal−organic frameworks (MOFs), the emerging hydrogen-bonded organic frameworks (HOFs) self-assembled from organic molecules via intermolecular hydrogen-bonding interactions represent a relatively new class of crystalline porous materials, which hold substantial potential to address industrially challenging gas separations.[8−14] HOFs are metal-free, lightweight, and feature nonpolar pores, making them particularly promising for the separation of noble gases and alkane-selective alkane/alkene separation. However, the relatively weak hydrogen-bonding connections in HOFs commonly lead to fragile frameworks, which may lose structural integrity and crystallinity upon activation or exposure to moisture.[15,16] Thus, it is very challenging yet vital to construct highly stable HOFs with desirable gas separation performance.

Structural interpenetration has been commonly observed in MOFs which can effectively enhance framework stability;[17,18] however, this has been rarely documented for HOFs. In this work, we report a microporous HOF, denoted as HIAM-103 (HIAM = Hoffmann Institute of Advanced Materials), assembled from a hexacarboxylate linker (2,4,6-trimethylbenzene-1,3,5-triylisophthalic acid, H_6TMBTI). It features a four-fold interpenetrated network with high stability. The 1D nonpolar channels demonstrate the selective adsorption of C_2H_6 over C_2H_4 and Xe over Kr. Binary mixture column breakthrough measurements confirmed the separation capability of the compound. DFT calculations revealed that the selective adsorption originates from the adsorbate-dependent interaction with the nonpolar pore surface.

Colorless rodlike crystals of HIAM-103 were obtained from solvothermal reactions by heating H_6TMBTI in formic acid at 150 °C for 2 days (see the Supporting Information for

Received: March 27, 2023
Revised: June 14, 2023
Accepted: June 14, 2023
Published: June 29, 2023

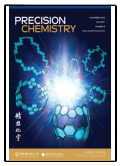

https://doi.org/10.1021/prechem.3c00040
Precis. Chem. 2023, 1, 524−529

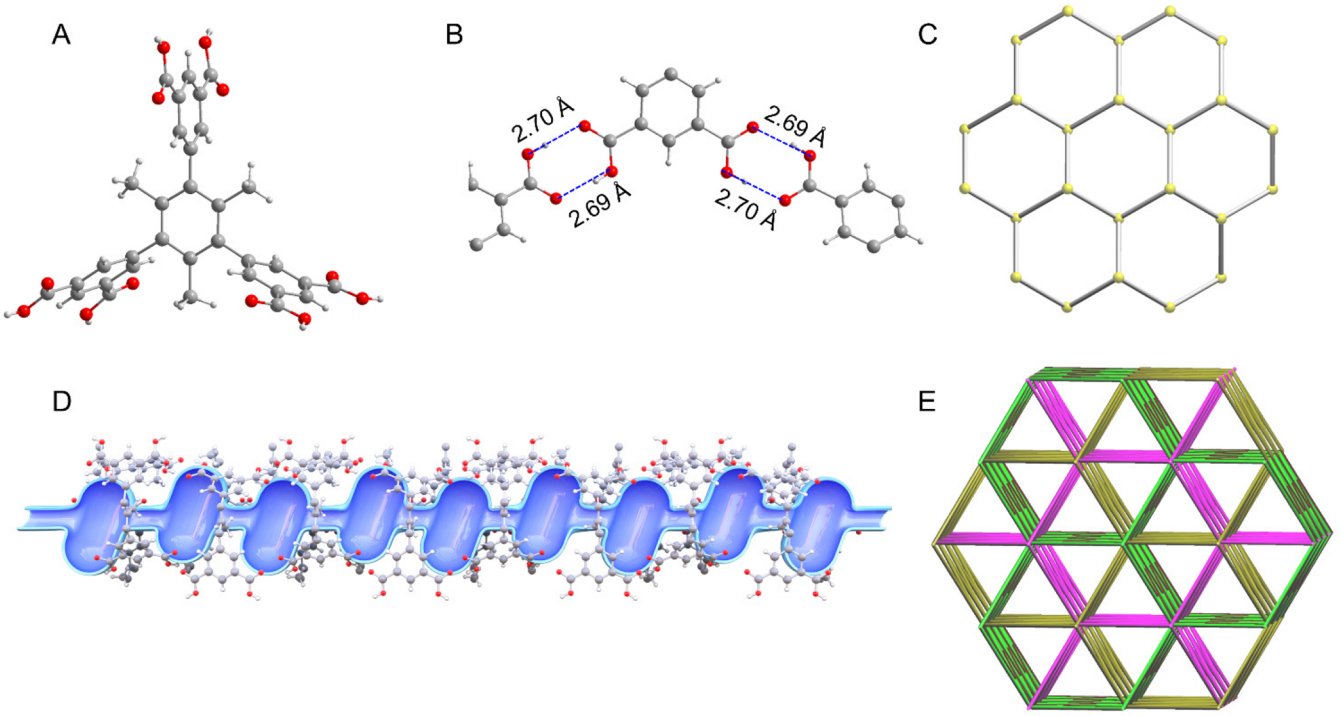

Figure 1. Structure of the HIAM-103. (A) Molecular structure of H_6TMBTI. (B) Hydrogen bonds between H_6TMBTI molecules in HIAM-103 (distances shown are between acceptor and donor oxygen atoms). (C) Crystal structure of HIAM-103 with four-fold interpenetration. (D) 1D segmented channel in HIAM-103. (E) Topology of HIAM-103, four identical nets are highlighted in different colors.

synthesis details, Figure S1). The structure was determined by single-crystal X-ray diffraction analysis. It crystallizes in the trigonal crystal system with a space group of *P*31*c* (Table S1). In the crystal structure, each H_6TMBTI building unit is connected to six neighboring units by 12 hydrogen bonds. The O−H···O angles and H-bonding distances (O−O) are 167.8/175.9° and 2.69/2.70 Å (Figure 1A,B), respectively, similar to those of the previously reported HOFs. The interconnection of H_6TMBTI leads to the formation of an **acs** type network. Four identical nets interpenetrate to form the resultant four-fold interpenetrated framework of HIAM-103 (Figure 1C−E). The final structure possesses 1D triangular segmented channels with a diameter of ∼6 Å decorated with abundant methyl groups. It should be noted that the crystal structure of HIAM-103 is different from the previously reported JLU-SOF3 and ZJU-HOF-1 which are also built on H_6TMBTI with three-fold interpenetrated networks (Figure S2, Table S3).

Phase purity of the as-synthesized HIAM-103 was confirmed by powder X-ray diffraction (PXRD) measurements, and the pattern matches well with the simulated one (Figure S3). Thermogravimetric analysis (TGA) showed that there is no weight loss up to 400 °C (Figure S4). The compound exhibits exceptional thermal and hydrothermal stability. Temperature-variable in situ XRD measurements indicated that the crystal structure remains intact up to 400 °C (Figure S5), consistent with the TGA results. Its crystallinity was also completely preserved after being heated at 150 °C in open air for 30 days or immersed in boiling water for 7 days (Figure S6). In addition, single crystals of HIAM-103 kept intact upon thermal activation, allowing us to precisely determine the crystal structure of the activated phase. Subsequent single-crystal X-ray diffraction analysis confirmed that the structure of activated HIAM-103 remains the same as that of the as-synthesized phase (Table S2). No notable sliding or distortion of the interpenetrated nets commonly observed in MOFs was detected in this case, indicating the robustness of the four-fold interpenetrated structure. Besides, the hydrophobicity of HIAM-103 was evaluated by water adsorption experiment at 298 K which showed a very small uptake (<1 mmol/g) up to P/P_0 = 1 (Figure S7).

Permanent porosity of HIAM-103 was analyzed by N_2 adsorption at 77 K (Figure S8). The compound exhibits a typical type-I adsorption profile with a saturated adsorption capacity of 194 cm^3/g. The calculated BET surface area and pore volume are 579 m^2/g and 0.306 cc/g, respectively. Pore size distribution curve derived from the N_2 adsorption isotherm displays a peak centered at 6 Å, in good agreement with the value measured from the crystal structure (Figure S9). As a result of higher order (four-fold) interpenetration, HIAM-103 has a decreased porosity and pore size compared to those of JLU-SOF3 and ZJU-HOF-1 (Table S3). In order to further verify the water stability of the material, a sample immersed in boiling water for 7 days was recovered and tested for nitrogen adsorption at 77 K. The results indicated no notable change was observed in adsorption capacity and BET surface area, suggesting its high resistance to water (Figure S8).

The highly robust structure, suitable pore dimensions, and nonpolar/hydrophobic channels of HIAM-103 prompted us to investigate its potential use in adsorptive separation of industrially important gases mixtures. We first looked into its adsorption toward ethane (C_2H_6) and ethylene (C_2H_4). The separation of C_2H_6 and C_2H_4 is of paramount importance in the petrochemical industry to produce polymer-grade C_2H_4. Recent research focus has shifted from C_2H_4-selective to C_2H_6-selective adsorbents as the latter would enable one-step C_2H_4 purification with a simplified separation process and reduced energy consumption.[19−22] Previous studies have demonstrated that nonpolar pores may be advantageous for favored

https://doi.org/10.1021/prechem.3c00040
Precis. Chem. 2023, 1, 524−529

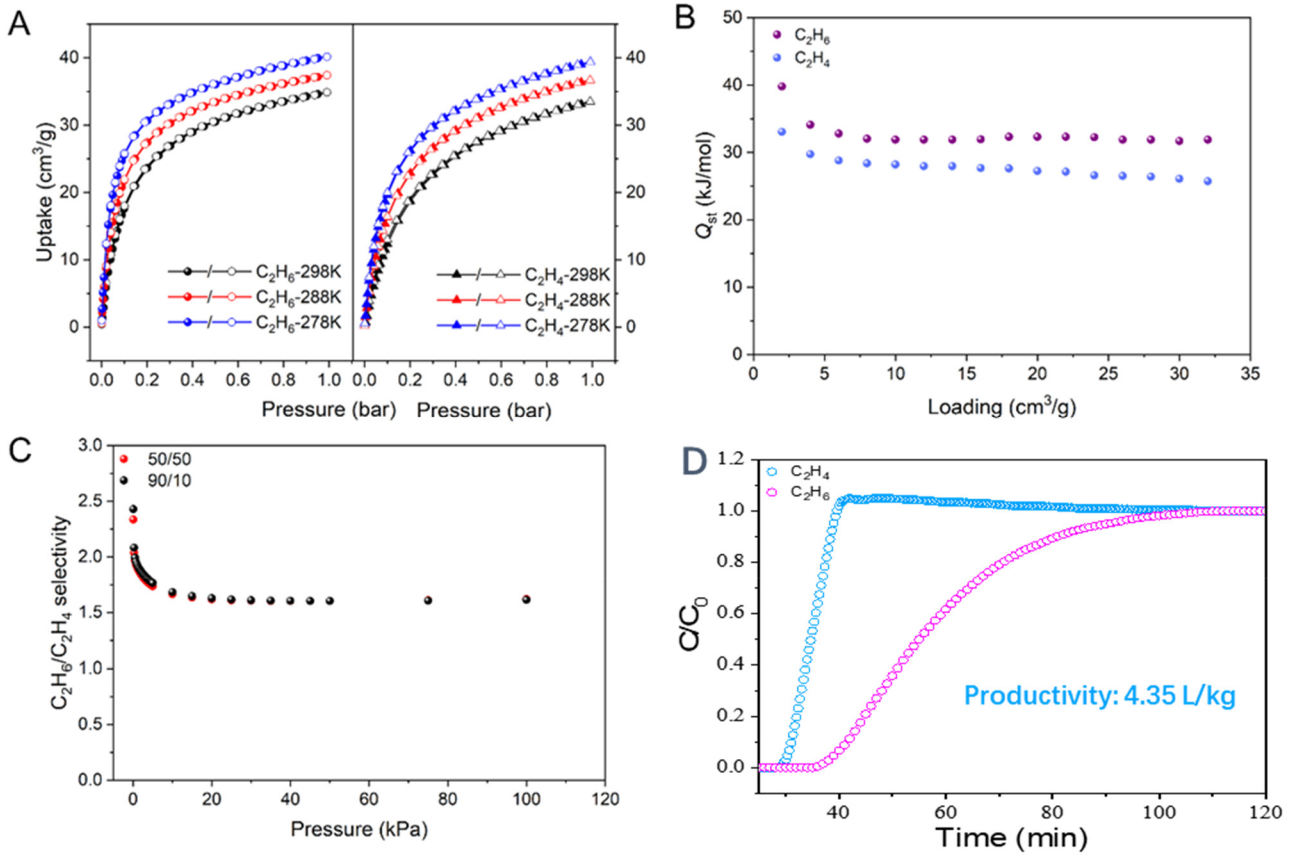

Figure 2. (A) Adsorption−desorption isotherms of C_2H_6 and C_2H_4 in HIAM-103 at 278, 288, and 298 K. (B) Isosteric heats of adsorption (Q_{st}) of C_2H_6 and C_2H_4 as a function of gas loading. (C) C_2H_6/C_2H_4 IAST selectivities as a function of pressure with compositions of C_2H_6/C_2H_4 = 90/10 and 50/50. (D) Breakthrough curves of the C_2H_6/C_2H_4 (90/10) binary mixture at 298 K.

adsorption of C_2H_6 over C_2H_4 as a result of stronger C_2H_6-sorbent interaction.[23]

Single-component adsorption isotherms of C_2H_6 and C_2H_4 were collected at 278, 288, and 298 K (Figure 2A). The adsorbed amounts of C_2H_6 at 1 bar are 40.16, 37.40, and 34.9 cm^3/g at 278, 288, and 298 K, respectively, higher than the values for C_2H_4 (39.4, 36.7, and 33.5 cm^3/g) under identical conditions, indicating its preferential adsorption of C_2H_6 over C_2H_4. The isosteric heats of adsorption (Q_{st}) for C_2H_6 and C_2H_4 as a function of gas loading are shown in Figure 2B, with initial values of 39.80 and 33.06 kJ/mol, respectively, again confirming the preferred adsorption of C_2H_6 over C_2H_4.

To quantitatively assess the selective adsorption of C_2H_6 over C_2H_4 by HIAM-103, ideal adsorbed solution theory (IAST) was applied to calculate C_2H_6/C_2H_4 selectivities of different compositions at 298 K. The results indicated at both compositions (C_2H_6/C_2H_4 = 90/10 and 50/50), C_2H_6/C_2H_4 adsorption selectivities were above 2.3 at low pressure and stabilized at 1.6 (Figure 2C). To further validate the separation capability of HIAM-103, column breakthrough measurements for binary mixtures of C_2H_6 and C_2H_4 were performed. For a binary mixture of C_2H_6/C_2H_4 = 90/10, which mimics industrial conditions, C_2H_4 eluted out at the 28th minute with high purity (>99.9%) while C_2H_6 was retained in the column for 35 min, allowing the direct production of highly pure C_2H_4 with a productivity of 4.35 L/kg (Figures 2D and S11). This result has verified the capability of HIAM-103 for the one-step purification of C_2H_4 from C_2H_6/C_2H_4 mixtures through selective adsorption of C_2H_6 over C_2H_4. Considering the importance of water resistance of adsorbents in real-world applications, we further carried out breakthrough measurements under humid conditions. The results show that essentially no loss of separation capability was observed for HIAM-103 under 60% RH, suggesting high stability of the compound in the presence of water (Figure S9).

Adsorption and separation of Xe and Kr by HIAM-103 were studied subsequently. Adsorption−desorption isotherms at 278, 288, and 298 K were collected for both Xe and Kr. The adsorbed amounts for Xe are 35.60, 33.47, and 31.14 cm^3/g at 278, 288, and 298 K, respectively, notably higher than those for Kr (16.4, 13.8, 11.4 cm^3/g) under identical conditions (Figure 3A). Heats of adsorption calculations indicated that the initial Q_{st} values for Xe and Kr are 24.5 and 9.7 kJ/mol (Figure 3B). This agrees well with the adsorption isotherms. Xe is noticeably favored over Kr by HIAM-103 as a result of its stronger interaction with the framework. IAST calculations were conducted by using adsorption isotherms at 278, 288, and 298 K to quantitatively evaluate the adsorption selectivity. Xe/Kr selectivity at 298 K for a Xe/Kr = 20/80 mixture was calculated to be 8.3 (Figure 3C), comparable to most of adsorbents reported for Xe/Kr separation.[2,24] Binary mixture column breakthrough experiments were carried out to verify the feasibility of using HIAM-103 for the separation of Xe and Kr. For a binary mixture of Xe/Kr = 20/80 at room temperature, Kr broke out first at the eighth minute. In contrast, Xe was retained in the column for a substantially longer time and did not elute out until the 36th min (Figure

https://doi.org/10.1021/prechem.3c00040
Precis. Chem. 2023, 1, 524−529

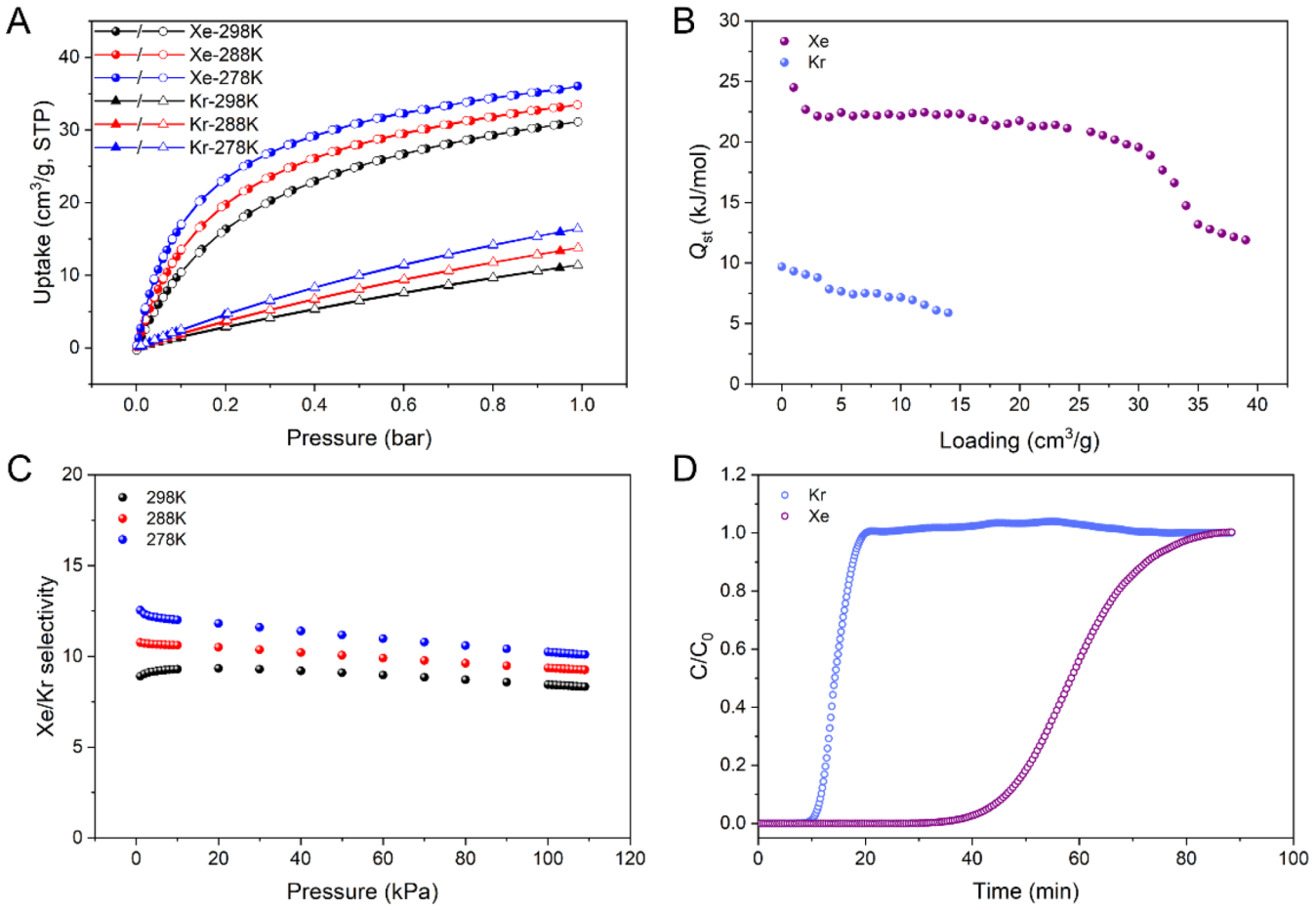

Figure 3. (A) Adsorption−desorption isotherms of Xe and Kr in HIAM-103 at 278, 288, and 298 K. (B) Q_{st} values of Xe and Kr as a function of gas loading. (C) Xe/Kr IAST selectivities as a function of pressure with a composition of Xe/Kr = 20/80 at different temperatures. (D) Breakthrough curves of the Xe/Kr (20/80) binary mixture at 298 K.

3D). These results confirm the ability of HIAM-103 for the efficient separation of Xe and Kr.

To explore the adsorption mechanism and the origin of the selective adsorption by HIAM-103, DFT calculations were performed for the accommodation of C_2H_4, C_2H_6, Kr, and Xe. Primary adsorption sites were located for all four gases with similar positions near the methyl groups of H_6TMBTI (Figure 4). It was observed that adsorbed C_2H_6 and C_2H_4 interact with the methyl groups through H···H bonding forces, with the shortest HC···CH distances of 4.10 and 4.94 Å for C_2H_6 and C_2H_4, respectively, leading to the calculated adsorption enthalpy of −0.35 and −0.31 eV for C_2H_6 and C_2H_4, respectively. These data are consistent with the experimental adsorption results, confirming the preferential adsorption of C_2H_6 over C_2H_4. Similar trend was found for Xe and Kr, with adsorption enthalpy of −0.25 and −0.20 eV for Xe and Kr, respectively, which again agree with the experimental adsorption results.

In summary, we have developed a new microporous HOF material and explored its capability for adsorption and separation of small gases, including C_2H_6/C_2H_4 and Xe/Kr. The HOF exhibits exceptional thermal and moisture stability as a result of its four-fold interpenetrated structure. Additionally, the methyl group decorated 1D channels contribute primarily to the selective adsorption of C_2H_6 over C_2H_4 and Xe over Kr. The separation capability was validated by binary mixture breakthrough measurements. The selective adsorption mechanism was analyzed by DFT calculations. This study demonstrates that HOFs with interpenetrated structures can effectively enhance their framework stability, and methyl groups play an important role in the separation selectivity via H-bonding interactions.

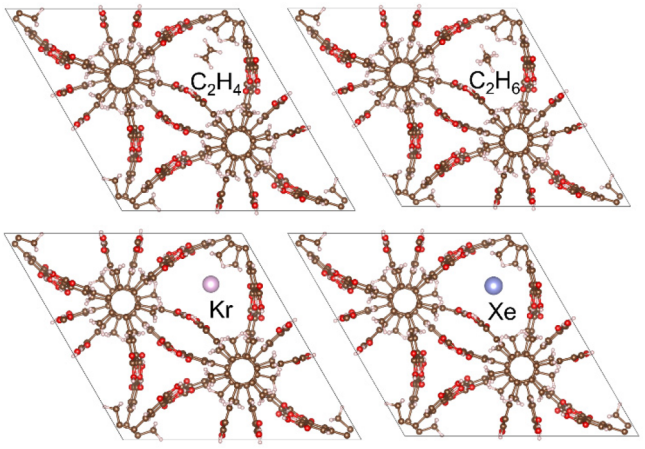

Figure 4. Optimized structure of C_2H_4, C_2H_6, Kr, and Xe loaded HIAM-103 showing the primary adsorption sites.

https://doi.org/10.1021/prechem.3c00040
Precis. Chem. 2023, 1, 524−529

■ ASSOCIATED CONTENT

Supporting Information

The Supporting Information is available free of charge at https://pubs.acs.org/doi/10.1021/prechem.3c00040.

Experimental details, PXRD data, N_2 adsorption isotherms, stability tests (PDF)

Crystallogrpahic data for activated HIAM-103 (CIF)

Crystallogrpahic data for HIAM-103 (CIF)

■ AUTHOR INFORMATION

Corresponding Authors

Hao Wang − *Hoffmann Institute of Advanced Materials, Shenzhen Polytechnic, Shenzhen 518055 Guangdong, P. R. China;* orcid.org/0000-0001-7732-778X; Email: wanghao@szpt.edu.cn

Jing Li − *Department of Chemistry and Chemical Biology, Rutgers University, Piscataway, New Jersey 08854, United States; Hoffmann Institute of Advanced Materials, Shenzhen Polytechnic, Shenzhen 518055 Guangdong, P. R. China;* orcid.org/0000-0001-7792-4322; Email: jingli@rutgers.edu

Authors

Fu-An Guo − *Hoffmann Institute of Advanced Materials, Shenzhen Polytechnic, Shenzhen 518055 Guangdong, P. R. China*

Kang Zhou − *Hoffmann Institute of Advanced Materials, Shenzhen Polytechnic, Shenzhen 518055 Guangdong, P. R. China*

Jiaqi Liu − *Hoffmann Institute of Advanced Materials, Shenzhen Polytechnic, Shenzhen 518055 Guangdong, P. R. China*

Complete contact information is available at: https://pubs.acs.org/10.1021/prechem.3c00040

Author Contributions

The manuscript was written through contributions of all authors.

Notes

The authors declare no competing financial interest.

■ ACKNOWLEDGMENTS

This work is financially supported by Shenzhen Science and Technology Program (No. RCYX20200714114539243, KCXFZ20211020163818026) and the U.S. Department of Energy, Office of Science, Office of Basic Energy Sciences, under Award No. DE-SC0019902.

■ REFERENCES

(1) Li, J.-R.; Sculley, J.; Zhou, H.-C. Metal-Organic Frameworks for Separations. *Chem. Rev.* **2012**, *112*, 869−932.

(2) Banerjee, D.; Cairns, A. J.; Liu, J.; Motkuri, R. K.; Nune, S. K.; Fernandez, C. A.; Krishna, R.; Strachan, D. M.; Thallapally, P. K. Potential of Metal-Organic Frameworks for Separation of Xenon and Krypton. *Acc. Chem. Res.* **2015**, *48*, 211−219.

(3) Adil, K.; Belmabkhout, Y.; Pillai, R. S.; Cadiau, A.; Bhatt, P. M.; Assen, A. H.; Maurin, G.; Eddaoudi, M. Gas/vapour separation using ultra-microporous metal−organic frameworks: insights into the structure/separation relationship. *Chem. Soc. Rev.* **2017**, *46*, 3402−3430.

(4) Sakai, M.; Sasaki, Y.; Tomono, T.; Seshimo, M.; Matsukata, M. Olefin Selective Ag-Exchanged X-Type Zeolite Membrane for Propylene/Propane and Ethylene/Ethane Separation. *ACS Appl. Mater. Interfaces* **2019**, *11*, 4145−4151.

(5) Narin, G.; Martins, V. F. D.; Campo, M.; Ribeiro, A. M.; Ferreira, A.; Santos, J. C.; Schumann, K.; Rodrigues, A. E. Light olefins/paraffins separation with 13X zeolite binderless beads. *Sep. Purif. Technol.* **2014**, *133*, 452−475.

(6) Luna-Triguero, A.; Sławek, A.; Sánchez-de-Armas, R.; Gutiérrez-Sevillano, J. J.; Ania, C. O.; Parra, J. B.; Vicent-Luna, J. M.; Calero, S. π-Complexation for olefin/paraffin separation using aluminosilicates. *Chem. Eng. J.* **2020**, *380*, 122482.

(7) Du, S.; Huang, J.; Ryder, M. R.; Daemen, L. L.; Yang, C.; Zhang, H.; Yin, P.; Lai, Y.; Xiao, J.; Dai, S.; Chen, B. Probing sub-5 Ångstrom micropores in carbon for precise light olefin/paraffin separation. *Nat. Commun.* **2023**, *14*, 1197.

(8) Hisaki, I.; Xin, C.; Takahashi, K.; Nakamura, T. Designing Hydrogen-Bonded Organic Frameworks (HOFs) with Permanent Porosity. *Angew. Chem., Int. Ed.* **2019**, *58*, 11160−11170.

(9) Wang, J.-X.; Gu, X.-W.; Lin, Y.-X.; Li, B.; Qian, G. A Novel Hydrogen-Bonded Organic Framework with Highly Permanent Porosity for Boosting Ethane/Ethylene Separation. *ACS Materials Lett.* **2021**, *3*, 497−503.

(10) Yang, J.; Wang, J.; Hou, B.; Huang, X.; Wang, T.; Bao, Y.; Hao, H. Porous hydrogen-bonded organic frameworks (HOFs): From design to potential applications. *Chem. Eng. J.* **2020**, *399*, 125873.

(11) Hu, F.; Liu, C.; Wu, M.; Pang, J.; Jiang, F.; Yuan, D.; Hong, M. An Ultrastable and Easily Regenerated Hydrogen-Bonded Organic Molecular Framework with Permanent Porosity. *Angew. Chem., Int. Ed.* **2017**, *56*, 2101−2104.

(12) Wang, H.; Li, B.; Wu, H.; Hu, T.-L.; Yao, Z.; Zhou, W.; Xiang, S.; Chen, B. A Flexible Microporous Hydrogen-Bonded Organic Framework for Gas Sorption and Separation. *J. Am. Chem. Soc.* **2015**, *137*, 9963−9970.

(13) Zhang, X.; Li, L.; Wang, J.-X.; Wen, H.-M.; Krishna, R.; Wu, H.; Zhou, W.; Chen, Z.-N.; Li, B.; Qian, G.; Chen, B. Selective Ethane/Ethylene Separation in a Robust Microporous Hydrogen-Bonded Organic Framework. *J. Am. Chem. Soc.* **2020**, *142*, 633−640.

(14) Zhang, X.; Wang, J.-X.; Li, L.; Pei, J.; Krishna, R.; Wu, H.; Zhou, W.; Qian, G.; Chen, B.; Li, B. A Rod-Packing Hydrogen-Bonded Organic Framework with Suitable Pore Confinement for Benchmark Ethane/Ethylene Separation. *Angew. Chem., Int. Ed.* **2021**, *60*, 10304−10310.

(15) Karmakar, A.; Illathvalappil, R.; Anothumakkool, B.; Sen, A.; Samanta, P.; Desai, A. V.; Kurungot, S.; Ghosh, S. K. Hydrogen-Bonded Organic Frameworks (HOFs): A New Class of Porous Crystalline Proton-Conducting Materials. *Angew. Chem., Int. Ed.* **2016**, *55*, 10667−10671.

(16) He, Y.; Xiang, S.; Chen, B. A Microporous Hydrogen-Bonded Organic Framework for Highly Selective C2H2/C2H4 Separation at Ambient Temperature. *J. Am. Chem. Soc.* **2011**, *133*, 14570−14573.

(17) Jiang, H.-L.; Makal, T. A.; Zhou, H.-C. Interpenetration control in metal−organic frameworks for functional applications. *Coord. Chem. Rev.* **2013**, *257*, 2232−2249.

(18) Gong, Y.-N.; Zhong, D.-C.; Lu, T.-B. Interpenetrating metal-organic frameworks. *CrystEngComm* **2016**, *18*, 2596−2606.

(19) Zeng, H.; Xie, X.-J.; Xie, M.; Huang, Y.-L.; Luo, D.; Wang, T.; Zhao, Y.; Lu, W.; Li, D. Cage-Interconnected Metal-Organic Framework with Tailored Apertures for Efficient C2H6/C2H4 Separation under Humid Conditions. *J. Am. Chem. Soc.* **2019**, *141*, 20390−20396.

(20) Yang, H.; Wang, Y.; Krishna, R.; Jia, X.; Wang, Y.; Hong, A. N.; Dang, C.; Castillo, H. E.; Bu, X.; Feng, P. Pore-Space-Partition-Enabled Exceptional Ethane Uptake and Ethane-Selective Ethane−Ethylene Separation. *J. Am. Chem. Soc.* **2020**, *142*, 2222−2227.

(21) Lin, R.-B.; Wu, H.; Li, L.; Tang, X.-L.; Li, Z.; Gao, J.; Cui, H.; Zhou, W.; Chen, B. Boosting Ethane/Ethylene Separation within Isoreticular Ultramicroporous Metal-Organic Frameworks. *J. Am. Chem. Soc.* **2018**, *140*, 12940−12946.

(22) Li, L.; Lin, R.-B.; Krishna, R.; Li, H.; Xiang, S.; Wu, H.; Li, J.; Zhou, W.; Chen, B. Ethane/ethylene separation in a metal-organic framework with iron-peroxo sites. *Science* **2018**, *362*, 443.
(23) Liu, J.; Miao, J.; Ullah, S.; Zhou, K.; Yu, L.; Wang, H.; Wang, Y.; Thonhauser, T.; Li, J. A Water-Resistant Hydrogen-Bonded Organic Framework for Ethane/Ethylene Separation in Humid Environments. *ACS Materials Lett.* **2022**, *4*, 1227−1232.
(24) Li, L.; Guo, L.; Zhang, Z.; Yang, Q.; Yang, Y.; Bao, Z.; Ren, Q.; Li, J. A Robust Squarate-Based Metal−Organic Framework Demonstrates Record-High Affinity and Selectivity for Xenon over Krypton. *J. Am. Chem. Soc.* **2019**, *141*, 9358−9364.

https://doi.org/10.1021/prechem.3c00040
Precis. Chem. 2023, 1, 524−529